JB
Journals.ASM.org

RNase III Controls the Degradation of *corA* mRNA in *Escherichia coli*

Boram Lim,[a] Se-Hoon Sim,[a] Minji Sim,[a] Kyungsub Kim,[a] Che Ok Jeon,[a] Younghoon Lee,[b] Nam-Chul Ha,[c] and Kangseok Lee[a]

School of Biological Sciences, Chung-Ang University, Seoul, Republic of Korea[a]; Department of Chemistry, KAIST, Daejeon, Republic of Korea[b]; and Department of Manufacturing Pharmacy, Pusan National University, Busan, Republic of Korea[c]

In *Escherichia coli*, the *corA* gene encodes a transporter that mediates the influx of Co^{2+}, Mg^{2+}, and Ni^{2+} into the cell. During the course of experiments aimed at identifying RNase III-dependent genes in *E. coli*, we observed that steady-state levels of *corA* mRNA as well as the degree of cobalt influx into the cell were dependent on cellular concentrations of RNase III. In addition, changes in *corA* expression levels by different cellular concentrations of RNase III were closely correlated with degrees of resistance of *E. coli* cells to Co^{2+} and Ni^{2+}. *In vitro* and *in vivo* cleavage analyses of *corA* mRNA identified RNase III cleavage sites in the 5′-untranslated region of the *corA* mRNA. The introduction of nucleotide substitutions at the identified RNase III cleavage sites abolished RNase III cleavage activity on *corA* mRNA and resulted in prolonged half-lives of the mRNA, which demonstrates that RNase III cleavage constitutes a rate-determining step for *corA* mRNA degradation. These findings reveal an RNase III-mediated regulatory pathway that functions to modulate *corA* expression and, in turn, the influx of metal ions transported by CorA in *E. coli*.

The degradation and processing of mRNA involve numerous *cis*- and *trans*-acting factors. Among them, the RNase III family of enzymes plays a pivotal role in the control of mRNA stability in both prokaryotes and eukaryotes (14, 26, 32, 38, 43, 45). All RNase III family members contain a characteristic RNase domain commonly called the RNase III domain. RNase III is encoded by the *rnc* gene in *Escherichia coli* and was the first double-stranded RNA endoribonuclease to be described (36). This enzyme requires Mg^{2+} to cleave phosphodiester bonds, creating 5′-phosphate and 3′-hydroxyl termini with an overhang of 2 nucleotides (nt) (9). Several *in vivo* mRNA substrates for *E. coli* RNase III have been identified, including *rnc* mRNA (5, 28), *pnp* mRNA (35), *bdm* mRNA (19, 38), and *proU* mRNA (16). However, an analysis of mRNA species whose abundance was downregulated by increased cellular RNase IIII activity indicated that nearly 100 mRNA species could be potential targets of RNase III (38).

The functional importance of the regulation of *E. coli* RNase III activity has been best characterized for its role in rRNA processing (6). Recent studies have further emphasized its role in the degradation of *bdm* and *proU* mRNAs in response to osmotic stress (16, 38). Those studies suggested that RNase III activity may contribute to the adaptation of *E. coli* cells to environmental changes by rapidly controlling the abundance of related mRNA species.

In a previous study, we found that the alteration of RNase III concentrations in the cell changed the steady-state levels of *corA* mRNA more dramatically than most other potential targets of RNase III (38). The *corA* gene was initially discovered by its cobalt resistance phenotype in *E. coli* (30). Its protein product, the CorA protein, and its homologous proteins are well conserved across kingdoms (17). The CorA protein has been characterized as a transporter for Mg^{2+} and Co^{2+} with high affinities of 15 to 20 μM and 20 to 40 μM, respectively (12, 13, 18, 39). The CorA protein can also transport Ni^{2+} with an affinity of 200 to 400 μM. The functional role of CorA in *Salmonella* species has been well studied, and those studies showed that the CorA protein is constitutively expressed in a manner independent of Mg^{2+} concentrations in the medium (39). In *Salmonella*, Mg^{2+} is also transported by MgtA and MgtB, which are required for growth in low concentrations of Mg^{2+} (40), and *E. coli* has only an MgtA homolog (46). However, a recent study showed that levels of the CorA protein increase in stationary-phase *Salmonella enterica* cells when grown in LB or N-minimal medium with low concentrations of Mg^{2+} (10 μM), although the CorA protein content does not correlate with the transport of Mg^{2+} and Ni^{2+}, indicating that an unknown mechanism regulates CorA function, which also affects virulence in mice (31).

In *E. coli* and *S. enterica*, the affinity of CorA for Ni^{2+} is in the toxic concentration range, which is much higher than physiologically optimal concentrations for either species. However, the transport of Ni^{2+} by CorA affects the sensitivity of *E. coli* to oxidative stress induced by the lactoperoxidase system (37), indicating that the transport of Ni^{2+} by CorA may be physiologically relevant.

While the physiological roles of CorA have been relatively well studied, the factors directly affecting the expression of the *corA* gene have not been identified. We investigated the functional role of RNase III activity in *corA* expression in *E. coli*, and we report experimental evidence showing that RNase III controls the degradation of *corA* mRNA by cleaving its 5′-untranslated region (5′-UTR), which in turn influences the influx of metal ions transported by CorA into the cell.

MATERIALS AND METHODS

Strains and plasmids. *E. coli* strain MG1655*rnc-14*::ΔTn*10* was constructed by the P1 transduction of the *rnc-14*::ΔTn*10* allele from *E. coli* strain HT115, which was obtained from Donald L. Court. MG1655*mgtA* and MG1655*rnc-14*::ΔTn*10mgtA* were constructed by deleting the open reading frame of *mgtA* in the genomic DNA of MG1655 and MG1655*rnc-14*::ΔTn*10* by using a procedure described previously (10). PCR primers were mgtA H1P1 (5′-TTCTGTACTGTTTCAGACAGTGCGGAGGGAC TCCTTCATATGAATATCCTCCTTA) and mgtA H2P2 (5′-CAATCTG AATCGGGGCTATCGTGCCCAGTTTATTCTGTGTAGGCTGGAGCTG CTTC). BW25113*corA* was obtained from the *E. coli* stock center at Yale

Received 21 January 2012 Accepted 10 February 2012
Published ahead of print 17 February 2012
Address correspondence to Kangseok Lee, kangseok@cau.ac.kr.
B.L. and S.-H.S. contributed equally to this work.
Supplemental material for this article may be found at http://jb.asm.org/.

doi:10.1128/JB.00099-12

University. To construct pCRS1, a DNA fragment containing the *corA* gene was amplified by using PCR primers corA-5′ (5′-ATGCGGCCGCG ATCACTCTAAGAGGACATT) and corA-3′ (5′-ATGCGGCCGCTTAC AACCAGTTCTTCCGCT). The products were then cloned into the NotI site in pCAT924 (23, 24), resulting in pCRS1. To construct pCRS1-MT, DNA fragments containing mutations at cleavage sites A and B in the *corA* mRNA were amplified by using the overlap extension PCR method, digested with NotI, and cloned into the NotI site in pCRS1. The PCR primers were corA reporter 1-R (5′-AAGGCTATCAGCAAAAAGGGATAGCCTCTGG AGTTGATCCTGGATGACA), corA reporter 2-F (5′-GGCTATCCCTTT TTGCTGATAGCCTTAGGGGTTGTCAGCGACCTCAATT), corA-5′, and corA-3′.

Measurement of optimal Mg^{2+} concentrations. *E. coli* strains MG1655, MG1655*mgtA*, MG1655*rnc-14*::Δ*Tn10*, MG1655*rnc-14*::ΔTn*10mgtA*, BW25113, and BW25113*corA* were grown in LB overnight and harvested. The bacterial pellets were washed three times with N-minimal medium and diluted 1:100 in the same medium containing 0, 1, 10, 100, and 1,000 μM $MgSO_4$. The cultures were grown for an additional 16 h, and the optical density (OD) of the cultures at 600 nm was measured.

Measurement of MIC. *E. coli* strains MG1655*rnc-14*::ΔTn*10* and MG1655*rnc-14*::ΔTn*10mgtA* harboring pKAN6B (48) or pRNC1 (38) were grown in LB overnight and harvested. The bacterial pellets were washed three times with N-minimal medium and diluted 1:100 in the same medium containing 1 mM $MgSO_4$ and various concentrations of $CoCl_2$ (0 to 50 μM in increments of 5 μM) or $NiCl_2$ (0 to 250 μM in increments of 25 μM). L-Arabinose (0.1%) was additionally added to the strains harboring pKAN6B and pRNC1 for the expression of 0× and 10× RNase III, respectively. For the expression of 1× RNase III, 0.1% D-arabinose and 0.0001% L-arabinose were additionally added to the strains harboring pRNC1. The cultures were grown for an additional 16 h, and the optical density at 600 nm (OD_{600}) was measured for each culture. The basal level of the OD_{600} (<0.02) was considered no growth, and the lowest concentration of $CoCl_2$ or $NiCl_2$ that completely inhibited growth was designated the MIC.

Measurement of cobalt content. Soluble extracts were obtained from *E. coli* strains MG1655 and MG1655*rnc-14*::ΔTn*10* that were grown in LB in the presence or absence of 200 μM cobalt chloride until the OD_{600} reached 0.8. The bacterial pellets were washed three times with buffer N at 4°C and lysed in 4 M guanidine hydrochloride buffer (pH 7.2) by sonication. The cobalt content was measured colorimetrically as previously described (29, 33).

Western blot analysis. Western blot analysis was carried out as previously described (20). Polyclonal antibodies to CorA were obtained from Michael E. Maguire. Specific proteins were imaged by using a VersaDoc 100 instrument (Bio-Rad, Hercules, CA) and quantified by using Quantity One (Bio-Rad).

Quantitative PCR and RT-PCR. Quantitative PCR was performed as previously described (19). *E coli* strains MG1655 and MG1655*rnc-14*::ΔTn*10* were grown in LB and harvested at an OD_{600} of 0.6 for the purification of total RNA. The primers used for *corA* were 5′-GACTGCGCGTACAATCTGAA and 5′-GCCAACTGTTCGATTTTGGT. The primers used for *mtgA* were 5′-TAACGCTGGGGATAGAAACG and 5′-GGCTCACCGCCTAACTG ATA. The procedure for reverse transcription (RT)-PCR analysis was described previously (47, 48). The primers used for *corA* were 5′-GATCAC TCTAAGAGGACATT and 5′-TTACAACCAGTTCTTCCGCT.

Northern blot analysis. Total RNA samples were prepared from cultures grown in LB (OD_{600} = 0.6) using an RNeasy miniprep kit (Qiagen) 0, 5, 10, and 20 s after the addition of rifampin (1 mg ml^{-1}). Twenty micrograms of the total RNA sample was denatured at 65°C for 10 min in a double volume of formamide-formaldehyde loading buffer and separated by electrophoresis on a 1.2% agarose gel containing 0.6 M formaldehyde. The procedure for Northern blot analysis was described previously (22). The random hexamer probes used for *corA* mRNA were synthesized by using a random-primed DNA labeling kit (Roche, Pleasanton, CA), in which the PCR products containing the coding region of *corA* were used as a template. Primers corA-5′ and corA-3′ were used.

***In vitro* cleavage analyses and primer extension analysis.** His-tagged RNase III purification and cleavage assays were performed as previously described (1). The 3′/5′-end-labeled transcripts were either 5′-end labeled with [γ-^{32}P]ATP (6,000 mCi $mmol^{-1}$) and T4 polynucleotide kinase (New England Biolabs) or 3′-end labeled with [5′-^{32}P]cytidine 3′,5′-biphosphate ([5′-^{32}P]pCp) (3,000 mCi $mmol^{-1}$) and T4 RNA ligase (New England Biolabs) and then separated on 6% polyacrylamide gels containing 8 M urea. The transcripts were eluted from the gel after mixing for 16 h in a buffer containing 30 mM Tris-HCl (pH 7.9), 10 mM NaCl, 0.1% sodium dodecyl sulfate, and 0.1 mM EDTA (pH 8.0). The transcripts were purified by using phenol-chloroform extraction and ethanol precipitation. One picomole labeled transcript was incubated with 5 ng of purified RNase III in the presence of 0.25 μg ml^{-1} of yeast tRNA (Ambion) and 20 U of RNase inhibitor (Takara, Otsu, Japan) in cleavage buffer (30 mM Tris-HCl [pH 7.9], 160 mM NaCl, 0.1 mM dithiothreitol [DTT], 0.1 mM EDTA [pH 8.0]). Cleavage reactions were initiated by the addition of 10 mM $MgCl_2$ to the mixture after 5 min of incubation at 37°C. Samples were removed at the time intervals indicated in the figure legends and mixed with an equal volume of gel loading buffer II (Ambion) containing 95% formamide, 18 mM EDTA, 0.025% SDS, 0.025% xylene cyanol, and 0.025% bromophenol blue. The samples were denatured at 65°C for 10 min and separated on a 12% polyacrylamide gel containing 8 M urea and 1× Tris-borate-EDTA (TBE). Primer extension analysis was performed by using the total RNA purified by phenol extraction and ethanol precipitation and hybridized with 5′-^{32}P-labeled primers. The following primers were used: corA-N-3′ (5′-TTGCGGCCGCAGACACAGGCGAAC TTTCC), corA-M-3′ (5′-TTGCGGCCGCAGACACAGGCGAACTTT CC), corA-UTR-157R (5′-AACAGCCTGACTCAGCGCGA), and corA-3′. RNA and labeled primers were annealed at 65°C for 15 min and then slowly cooled down to 37°C for 1 to 2 h. They were then extended at 42°C for 1 h by using avian myeloblastosis virus (AMV) reverse transcriptase (New England Biolabs). The extended fragments were separated on 12% polyacrylamide gels as described above.

RESULTS

RNase III negatively regulates *corA* gene expression. To confirm the results of microarray analyses from our previous research (38), we measured steady-state levels of *corA* mRNA in wild-type and *rnc*-deleted cells of *E. coli* strain MG1655 using quantitative real-time PCR. Consistent with the microarray data, wild-type cells expressing RNase III (1× RNase III) demonstrated an approximately 4.5-fold decrease in the amount of *corA* mRNA compared with the amount in *rnc*-deleted cells (0× RNase III) (Fig. 1A). In wild-type cells that adventitiously overexpressed RNase III at levels 10 times the endogenous level (10× RNase III) from plasmid pRNC1 (35), the amount of *corA* mRNA was further decreased by 2.6-fold compared with the amount in wild-type cells harboring an empty vector (pKAN6B). Western blot analysis also showed that levels of CorA expression were well correlated with cellular concentrations of RNase III. Levels of CorA expression in the *rnc*-deleted cells were approximately 3 and 5 times higher than those in wild-type cells harboring pKAN6B and pRNC1, respectively (Fig. 1B). The difference in expression levels of the *corA* mRNA and the CorA protein was greater between *E. coli* cells expressing 0× and 1× RNase III than that between *E. coli* cells expressing 1× and 10× RNase III. We think that this discrepancy stems from the saturation of RNase III activity on *corA* expression in *E. coli* cells expressing 1× RNase III. Our previous study showed that expression levels of RNase III at levels 0.1 to 10.0 times the endogenous levels do not greatly affect the abundance of RNase III-targeted mRNA species and normal cellular growth in rich medium (36).

Next, we tested whether cellular levels of RNase E, a single-stranded RNA-specific endoribonuclease E, affect the *corA* mRNA abundance, since it is known to play a major role in mRNA decay

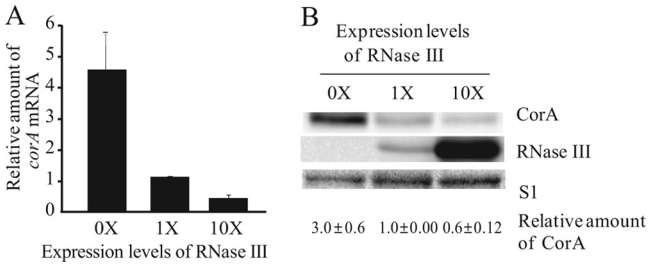

FIG 1 Downregulation of *corA* expression by RNase III. (A) Effects of the cellular RNase III concentration on *corA* mRNA levels were measured by using quantitative PCR analysis. Total RNA was prepared from *E. coli* strain MG1655, harboring pKAN6B or pRNC1, and MG1655*rnc-14*::ΔTn*10*, harboring pKAN6B. We measured the relative abundance of *corA* mRNA by setting the amount of *corA* mRNA in MG1655 cells harboring pKAN6B to 1. Levels of *mtgA* mRNA, which were independent of the cellular concentrations of RNase III (38), were used to normalize the amount of *corA* mRNA. (B) Western blot analysis of the CorA protein. *E. coli* strains MG1655, harboring pKAN6B or pRNC1, and MG1655*rnc-14*::ΔTn*10*, harboring pKAN6B, were grown in LB at 37°C to an OD_{600} of 0.8 to obtain total proteins. The amounts of CorA, RNase III, and ribosomal protein S1 were analyzed by using Western blot analyses. The S1 protein was used to provide an internal standard to evaluate the amount of cell extract in each lane. The same membrane probed for CorA was also probed with polyclonal antibodies to RNase III and S1.

in *E. coli* (2, 7, 25). We utilized *E. coli* strain KSL2000 (22), in which the chromosomal *rne* gene has been deleted and complemented with a construct that expresses RNase E from an *rne* gene under the arabinose-inducible P_{BAD} promoter in plasmid pBAD-RNE. In strain KSL2000, RNase E expression is controlled solely by the concentration of arabinose, and cellular RNase E levels can be conditionally knocked down to ~10% of endogenous RNase E levels without significantly affecting normal cellular growth. Steady-state levels of *corA* mRNA and the CorA protein were measured in KSL2000 cells in either the presence or the absence of arabinose. The results revealed no significant changes in expression levels of *corA* mRNA or the CorA protein in cells depleted of RNase E compared with cells that expressed endogenous levels of RNase E (see Fig. S1 in the supplemental material). These results demonstrate that RNase E is not actively involved in the decay pathway of *corA* mRNA.

RNase III affects the transport activity of CorA. We wished to test whether alterations in the levels of CorA expression are physiologically relevant to its normal function in *E. coli* by measuring the degree of resistance of *E. coli* cells expressing 0×, 1×, or 10× RNase III to Co^{2+} and Ni^{2+}. An excessive influx of Co^{2+} and Ni^{2+} by CorA inhibits normal cellular growth in *E. coli*. Cobalt toxicity is due mainly to its competition with iron in iron-containing proteins such as Fe-S clusters (33, 41) or via the cobalt-mediated oxidative stress of free-thiol pools (41), whereas nickel toxicity is likely to be related to nickel-mediated oxidative stress (35). For this reason, we expected that decreased expression levels of the CorA protein would result in the transport of smaller amounts of cobalt and nickel into the cell, which would consequently render *E. coli* cells more resistant to cobalt and nickel. First, we measured optimal Mg^{2+} concentrations for the growth of *mgtA*-deleted *E. coli* cells in order to circumvent indirect effects of MgtA, another putative Mg^{2+} transporter in *E. coli*, on the degree of resistance of *E. coli* cells to cobalt by different expression levels of CorA. Under Mg^{2+} concentrations equal to or below 10 μM, the growth of *mgtA*-deleted *E. coli* cells was inhibited (Fig. 2A), indicating an important functional role of MgtA in Mg^{2+} transport under Mg^{2+}-limited conditions. We obtained analogous results when an *mgtA* deletion was introduced into an *rnc*-deleted *E. coli* strain (Fig. 2B). As was shown previously for CorA function in magnesium transport in *Salmonella* species (29, 37, 38), the *corA* deletion did not affect the cellular growth of *E. coli* under Mg^{2+}-limited conditions (Fig. 2C). BW25113 and BW25113*corA* were used

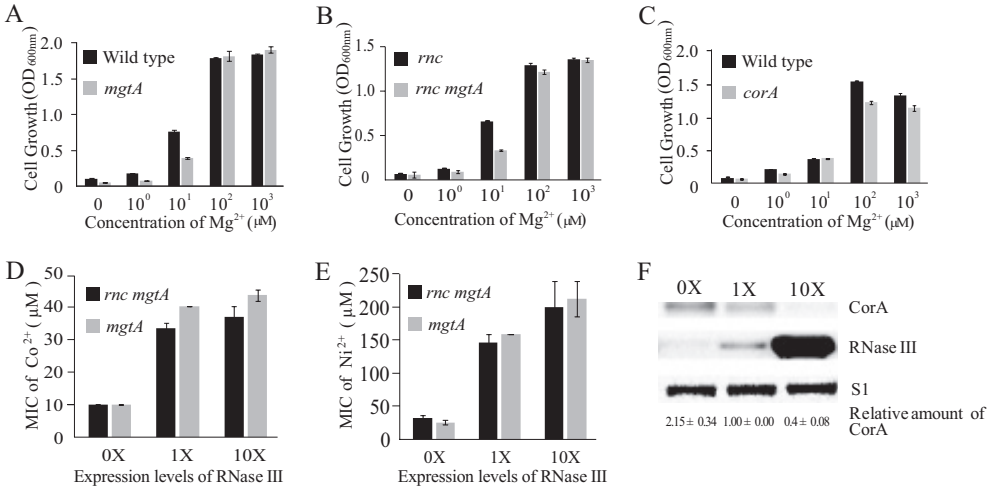

FIG 2 Effects of RNase III on transport activity of CorA. (A) Effects of an *mgtA* deletion on Mg^{2+}-dependent *E. coli* growth. (B) Effects of an *mgtA* deletion on the Mg^{2+}-dependent growth of *E. coli* cells deleted for *rnc*. (C) Effects of a *corA* deletion on Mg^{2+}-dependent *E. coli* growth. The Mg^{2+}-dependent growth rates between MG1655 and MG1655*mgtA*, MG1655*rnc-14*::ΔTn*10*, and MG1655*rnc-14*::ΔTn*10mgtA* (B) and BW25113 and BW25113*corA* (C) were compared. (D and E) Effects of expression levels of CorA modulated by RNase III on the degree of *E. coli* resistance to cobalt (D) or nickel (E). Activities of CorA were determined by the degree of resistance of *E. coli* strain MG1655*rnc-14*::ΔTn*10* harboring pKAN6B or pRNC1 to $CoCl_2$ (D) or $NiCl_2$ (E). MIC measurements were independently performed in triplicate in cells cultured in N-minimal medium supplemented with 1 mM $MgSO_4$ containing various concentrations of $CoCl_2$ (D) or $NiCl_2$ (E), and the values are shown along with means ± standard errors of the means. (F) Western blot analysis of the CorA protein. *E. coli* strain MG1655*rnc-14*::ΔTn*10* harboring pKAN6B or pRNC1 was grown in N medium supplemented with 1 mM $MgSO_4$ at 37°C to an OD_{600} of 0.3 to obtain total protein amounts. The same procedure as that described in the legend of Fig. 1B was used for Western blot analyses. Detailed experimental procedures are provided in Materials and Methods.

TABLE 1 Cobalt contents in wild-type and *rnc* strains

Strain and condition	Mean intracellular cobalt content (μM) ± SD[a]
MG1655	
$-Co^{2+}$	5.0 ± 0.0
$+Co^{2+}$ (200 μM)	11.3 ± 0.1
MG1655*rnc-14*::ΔTn*10*	
$-Co^{2+}$	17.2 ± 0.1
$+Co^{2+}$ (200 μM)	21.4 ± 0.3

[a] The cobalt content was determined by using a colorimetric assay (25). The cobalt contents for *corA*-deleted *E. coli* cells (BW25113*corA*) were 3.6 ± 0.1 μM (without Co^{2+}) and 5.4 ± 0.1 μM (with Co^{2+}).

for measurements of optimal Mg^{2+} concentrations because BW25113 is an *E. coli* strain that is very closely related to MG1655 (3, 4), and we were unable to obtain an MG1655-derived strain lacking *corA* despite several attempts to construct the strain.

Based on the results described above, we measured the MICs of cobalt and nickel for *E. coli* cells expressing 0×, 1×, or 10× RNase III in N-minimal medium supplemented with 1 mM $MgSO_4$. The MIC of cobalt for *E. coli* cells expressing 0× RNase III was 10.0 μM, whereas the MICs were 33.3 and 40.0 μM for *E. coli* cells expressing 1× and 10× RNase III, respectively (Fig. 2D). The MIC of nickel for *E. coli* cells expressing 0× RNase III was 33.3 μM, whereas the MICs were 160.0 and 240.0 μM for *E. coli* cells expressing 1× and 10× RNase III, respectively (Fig. 2E). The MICs were not significantly changed when *E. coli* cells deleted for *mgtA* were tested (Fig. 2D and E), indicating that MgtA expression in *E. coli* is suppressed in the presence of 1 mM Mg^{2+}, as was shown previously for that in *Salmonella* (39). The difference in MICs was greater between *E. coli* cells expressing 0× and 1× RNase III than that between *E. coli* cells expressing 1× and 10× RNase III. This discrepancy is probably due to a slightly slow growth phenotype of *E. coli* cells expressing 0× RNase III (Fig. 2B) and a saturation of RNase III activity upon *corA* expression in *E. coli* cells expressing 1× RNase III. Nonetheless, these results demonstrate the correlation between levels of CorA expression and the degree of resistance to cobalt and nickel. Expression levels of CorA were also closely correlated with cellular concentrations of RNase III under the conditions of MIC measurement (Fig. 2F).

To confirm that expression levels of the CorA protein directly affect cobalt accumulation, we used a colorimetric assay method to measure cobalt concentrations in wild-type and *rnc*-deleted *E. coli* cells that were grown to the mid-log phase in LB for 30 min in the presence or absence of an additional 200 μM $CoCl_2$. Among cells that were grown in LB without the addition of $CoCl_2$, the cobalt content in *rnc*-deleted *E. coli* cells was approximately three times higher than that in the wild-type cells (17.2 μM versus 5.0 μM) (Table 1). Among cells exposed to 200 μM $CoCl_2$, cobalt concentrations were 11.3 μM in wild-type cells and 21.4 μM in *rnc*-deleted cells (Table 1). These results indicate that different levels of CorA expression in isogenic *E. coli* strains differing in the *rnc* gene affect cobalt accumulation.

Identification of RNase III cleavage sites in *corA* mRNA. The correlation between steady-state levels of *corA* mRNA and cellular concentrations of RNase III suggests the presence of *cis*-acting elements in *corA* mRNA that are responsive to RNase III. To identify RNase III cleavage sites in *corA* mRNA, we performed primer extension experiments using several 5′-^{32}P-end-labeled primers and total RNA purified from wild-type and *rnc*-deleted cells. We observed two distinct cDNA bands that were present only in the lanes loaded with cDNA products from the reaction mixture containing total RNA from wild-type cells (Fig. 3A, bands A and B). In addition, these cDNA bands were more distinct when the reaction was carried out with total RNA prepared from *E. coli* cells that adventitiously overexpressed *corA* mRNA and RNase III (Fig. 3A, last lane). These cDNA bands corresponded to sites that were positioned in the double-stranded region in the 5′-UTR of the *corA* mRNA (Fig. 3B). RNase III cleavage at these sites was predicted to produce cleavage products with an overhang of 2 nucleotides at the 3′ end, which is characteristic of RNase III cleavage products. These sites were designated cleavage sites A and B.

The cleavage of *corA* mRNA by RNase III at cleavage sites A and B was further demonstrated biochemically by using an *in vitro*-synthesized model hairpin RNA and purified RNase III. The model hairpin RNA has a nucleotide sequence between nt −232 and −41 from the start codon of *corA*, which encompasses RNase III cleavage sites A and B in the *corA* mRNA (Fig. 3C). The RNase III cleavage of a 5′-^{32}P-end-labeled model hairpin RNA *in vitro* generated one major and one minor cleavage product, the lengths of which corresponded to cleavage sites A and B, respectively. The predicted secondary structure of the hairpin was confirmed by analyzing the cleavage patterns of the model hairpin RNA after RNase T1 and V1 digestion. Other minor cleavage products might have resulted from the intrinsic property of RNase III to randomly cleave RNA transcripts *in vitro* when the RNase III concentration is relatively high (44).

The radioactivity in the cleavage product at site A was ~12 times higher than that at site B. There are two possible explanations for this result. Either RNase III cleaves more efficiently at site A than at site B, or the cleavage product at site A appeared to be more abundant because the model hairpin was 5′-^{32}P-end labeled and the cleavage product at site A accumulated during the cleavage reaction. To address this uncertainty, we synthesized a 3′-^{32}P-end-labeled model hairpin and performed an *in vitro* cleavage assay. The results demonstrated that cleavage products at both sites were similarly accumulated, indicating that RNase III cleaves more efficiently at site A than at site B (Fig. 3D).

RNase III cleavage at sites A and B is a rate-limiting step for *corA* degradation. To test whether RNase III cleavage at sites A and B is a rate-limiting step for *corA* degradation, we introduced nucleotide substitutions (C-122G, U-153A, and A-152G) at the RNase III cleavage sites (Fig. 4A) in a *corA* overexpression plasmid (pCRS1). Wild-type and mutant *corA* mRNAs were expressed in *E. coli* cells lacking *corA*, and the half-lives of this mRNA and the cleavage specificity of RNase III were investigated. These nucleotides were created because they do not alter the overall secondary structure of the 5′-UTR of the *corA* mRNA. In addition, our previous research on RNase III cleavage site selection on *bdm* mRNA showed that base substitutions at scissile-bond sites are sufficient to alter RNase III cleavage activity (15). The half-life of the mutant mRNA more than doubled (~7 versus ~20 s), and RNase III was not able to efficiently cleave mutant *corA* mRNA at cleavage sites A and B *in vivo*, resulting in an increased expression level of the CorA protein from the mutant *corA* mRNA (Fig. 4B to D). These results demonstrate that RNase III cleavage at sites A and B is a rate-limiting step for *corA* degradation *in vivo*. The blocking of the RNase III cleavage of *corA* mRNA by the nucleotide substitution mutations in the *corA* mRNA was further demonstrated biochem-

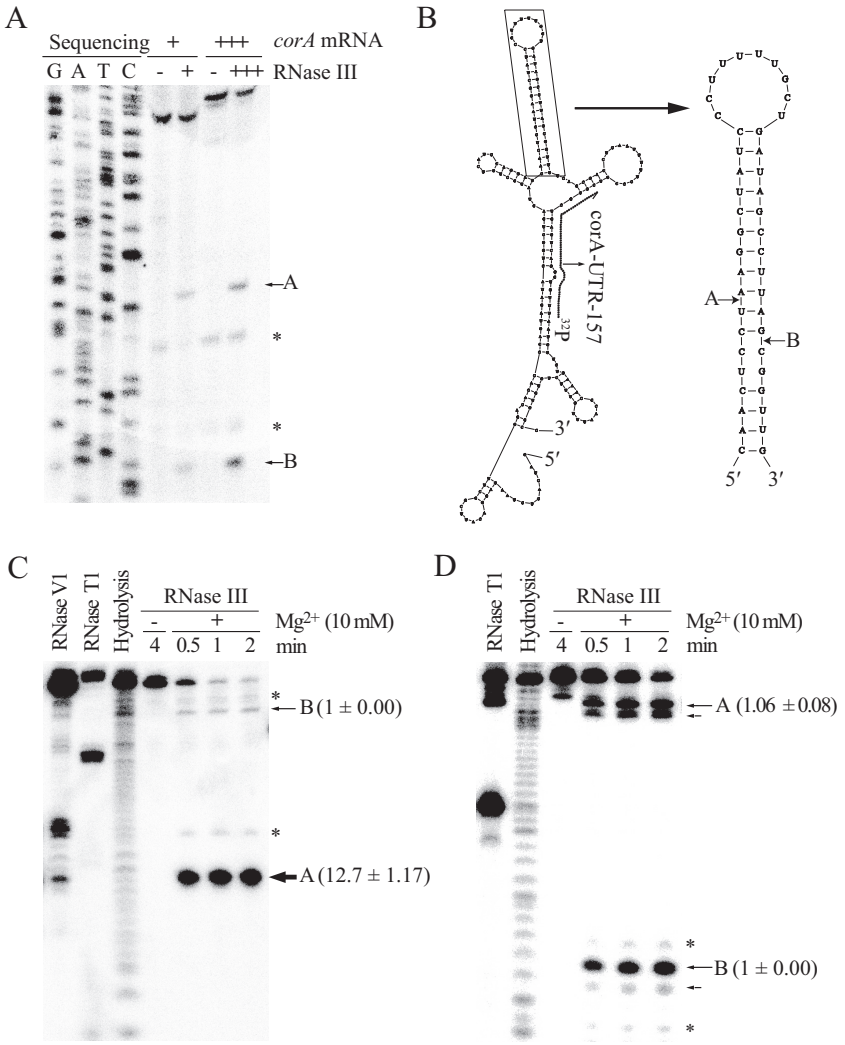

FIG 3 Identification of RNase III cleavage sites in *corA* mRNA *in vitro* and *in vivo*. (A) Primer extension analysis of *corA* mRNA synthesized *in vivo*. Total RNA was prepared from MG1655 and MG1655*rnc-14*::ΔTn*10* cells grown in LB (OD_{600} = 0.6) that endogenously (total 100 μg) or adventitiously (pCRS1) overexpressed (total, 50 μg) *corA* mRNA and hybridized with a 5′-end-labeled primer (corA UTR-157). Synthesized cDNA products were analyzed on a 12% polyacrylamide gel. Sequencing ladders were produced by using the same primer as that used for cDNA synthesis and PCR DNA encompassing the *corA* gene as a template. (B) Predicted secondary structure of *corA* mRNA. The secondary structure was deduced by using the M-fold program and RNase T1 and V1 digestion, as shown in panels C and D. The model hairpin RNA used for *in vitro* cleavage assays is shown in the right panel. (C and D) *In vitro* cleavage of the model *corA* hairpin RNA. One picomole the 5′-^{32}P-end-labeled (C) or 3′-^{32}P-end-labeled (D) *corA* model hairpin was incubated with 5 ng (~0.2 pmol) of purified RNase III in a cleavage buffer with $MgCl_2$ or without $MgCl_2$. Samples were withdrawn at the indicated time intervals and separated on 12% polyacrylamide gels containing 8 M urea. Cleavage products (A and B) were identified by using size markers generated by alkaline hydrolysis. The relative amounts of cleaved products A and B are indicated in parentheses as well as by the sizes of the arrows. Other cleavage products, whose sizes are shorter by 1 nt than those of the expected products (indicated with short arrows in panel D), might have resulted from the RNase III digestion of RNA transcripts containing a 1-nt deletion at the 3′ end. Other minor cleavage products are indicated with asterisks.

ically by using an *in vitro*-synthesized model hairpin RNA containing the corresponding mutations and purified RNase III. The results showed that RNase III was unable to cleave the model hairpin RNA containing the mutations (Fig. 4E).

DISCUSSION

We investigated the functional role of RNase III in the regulation of *corA* expression in *E. coli* and identified an RNase III-mediated regulatory pathway that controls *corA* expression. *In vitro* and *in vivo* analyses of *corA* mRNA revealed that RNase III controls the degradation of *corA* mRNA by cleaving the 5′-UTR, which consequently affects levels of CorA protein expression (Fig. 1 and 3). The blocking of the RNase III cleavage of *corA* mRNA by nucleotide substitution mutations at the cleavage site in the *corA* mRNA further demonstrated that RNase III cleavage is a rate-limiting step for *corA* degradation (Fig. 4). In addition, we showed that the downregulation of *corA* expression by RNase III results in the reduced accumulation of cobalt, which renders *E. coli* cells more resistant to cobalt stress (Fig. 2D and Table 1). The downregulation of *corA* expression by RNase III also rendered *E. coli* cells more resistant to nickel (Fig. 2E). As was shown previously for CorA function in Mg^{2+}

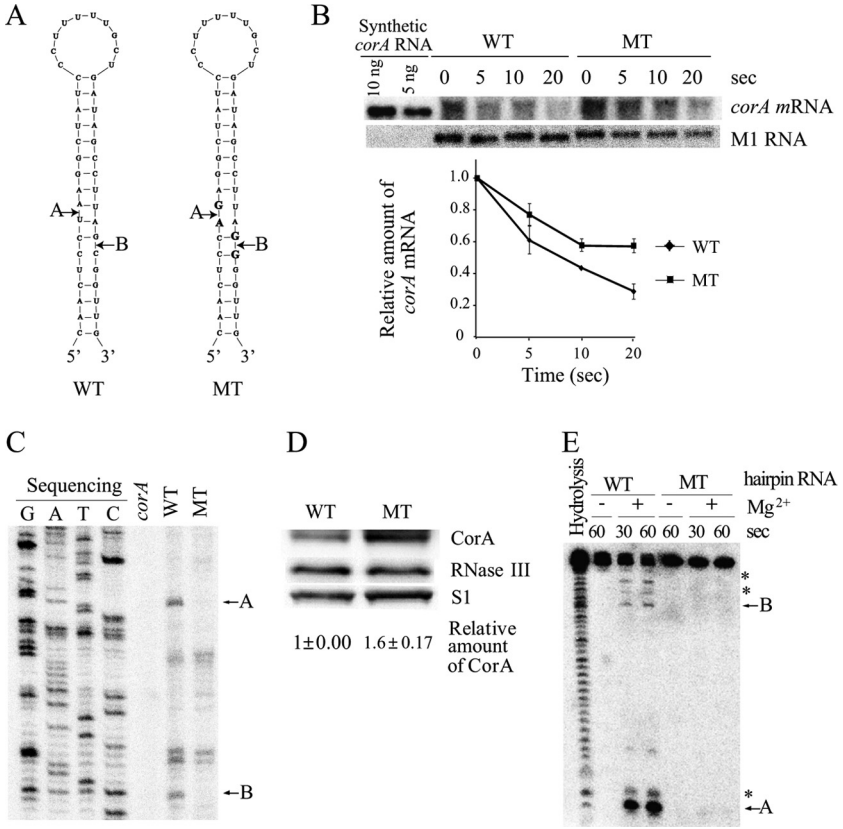

FIG 4 Inhibition of RNase III cleavage of *corA* mRNA by introduction of mutations at the cleavage site. (A) Secondary structures of the hairpin encompassing RNase III cleavage sites. Nucleotide substitutions (C-122G, U-153A, and A-152G) at the RNase III cleavage sites are shown. (B) Effects of mutations at the RNase III cleavage sites on *corA* mRNA decay. Plasmid pCRS1-MT expresses *corA* mRNA containing nucleotide substitutions (C-122G, U-153A, and A-152G) at the RNase III cleavage sites. Strain BW25113 deleted for *corA* (BW25113*corA*) and harboring either pCRS1-WT or pCRS1-MT was grown in LB at 37°C to an OD_{600} of 0.6. Total RNA samples were prepared from the cultures 0, 5, 10, and 20 s after the addition of rifampin (1 mg ml^{-1}) and separated on 1.2 M agarose gels containing 0.6 M formaldehyde. The abundances of *corA* mRNA and M1 RNA, the RNA component of RNase P (21, 34), were measured by Northern blotting with 5′-end-labeled primers. The abundance of M1 RNA was measured to provide an internal standard for evaluating the total amount of RNA in each lane. (C) Effects of mutations at the cleavage sites on RNase III cleavage activity on the *corA* mRNA. Total RNA was prepared from BW25113*corA* cells harboring no plasmid, pCRS1, or pCRS1-MT and analyzed as described in the legend of Fig. 3A. (D) Effects of mutations at the cleavage sites on levels of CorA protein expression. Total proteins were prepared from BW25113*corA* harboring no plasmid, pCRS1, or pCRS1-MT and analyzed as described in the legend of Fig. 1B. (E) Effects of mutations at the cleavage site on RNase III cleavage activity *in vitro*. A mutant model hairpin (MT) containing nucleotide substitutions (C-122G, U-153A, and A-152G) was synthesized and tested for RNase III activity on the RNA, as described in the legend of Fig. 3C. Cleavage products at RNase III sites A and B are shown with arrows, and other minor cleavage products are indicated with asterisks.

transport in *Salmonella* species (29, 38), the *corA* deletion did not affect the cellular growth of *E. coli* under Mg^{2+}-limited conditions (Fig. 2C). These results highlight the physiological significance of the regulation of *corA* expression.

The rapid degradation of *corA* mRNA by RNase III cleavage is not likely to stem from differences in translation efficiencies between the intact and the RNase III-cleaved *corA* mRNAs because the RNase III cleavage site is distant from the putative ribosome binding site. In addition, RNase III cleavage does not appear to change the RNA structure of the region encompassing the putative ribosome binding site of the *corA* mRNA (Fig. 1B). Rather, we hypothesize that the removal of the 5′ hairpin by RNase III cleavage generates *corA* mRNA that is vulnerable to attack by RNases, the action of which is inhibited by the presence of 5′ hairpins and/or a triphosphate group at the 5′ end of the mRNA (11, 15, 27, 42).

Unlike the regulation of RNase III activity on *bdm* and *proU* mRNAs in response to osmotic stress (38), RNase III activity on the *corA* mRNA was not significantly altered in *E. coli* cells subjected to cobalt or nickel stress (see Fig. S2 in the supplemental material). These results indicate that RNase III does not directly control *corA* expression in response to cobalt/nickel stress, at least under the conditions tested. However, it is possible that under different environmental conditions, another regulatory pathway exists to modulate RNase III activity on *corA* and other mRNA species that encode factors related to CorA activity and/or RNase III activity upon cobalt/nickel stress. This view is supported by the observation that RNase III activity on *pnp* mRNA, which is a well-characterized *in vivo* RNase III substrate (32), is upregulated in *E. coli* cells exposed to cobalt stress (our unpublished data). It was also shown that the PhoPQ gene status has an effect on the activity of the CorA protein (8), the mechanism of which has not yet been characterized. The identification of these factors and conditions will advance our understanding of the role of RNase III in modulating rapid physiological adjustments to environmental changes, such as metal stress.

ACKNOWLEDGMENTS

We thank Michael E. Maguire for providing antibodies to CorA to us.

This work was supported by NRF grants (2011-0028553 and 2010-0029167) funded by the Ministry of Education, Science, and Technology, Republic of Korea.

REFERENCES

1. **Amarasinghe AK, Calin-Jageman I, Harmouch A, Sun W, Nicholson AW.** 2001. *Escherichia coli* ribonuclease III: affinity purification of hexahistidine-tagged enzyme and assays for substrate binding and cleavage. Methods Enzymol. **342**:143–158.
2. **Apirion D.** 1975. The fate of mRNA and rRNA in *Escherichia coli.* Brookhaven Symp. Biol. **1975**:286–306.
3. **Baba T, et al.** 2006. Construction of *Escherichia coli* K-12 in-frame, single-gene knockout mutants: the Keio collection. Mol. Syst. Biol. **2**:2006.0008.
4. **Bachmann BJ.** 1972. Pedigrees of some mutant strains of *Escherichia coli* K-12. Bacteriol. Rev. **36**:525–557.
5. **Bardwell JC, et al.** 1989. Autoregulation of RNase III operon by mRNA processing. EMBO J. **8**:3401–3407.
6. **Bram RJ, Young RA, Steitz JA.** 1980. The ribonuclease III site flanking 23S sequences in the 30S ribosomal precursor RNA of *E. coli.* Cell **19**:393–401.
7. **Carpousis AJ.** 2007. The RNA degradosome of *Escherichia coli*: an mRNA-degrading machine assembled on RNase E. Annu. Rev. Microbiol. **61**:71–87.
8. **Chamnongpol S, Groisman EA.** 2002. Mg^{2+} homeostasis and avoidance of metal toxicity. Mol. Microbiol. **44**:561–571.
9. **Court DL.** 1993. RNA processing and degradation by RNase III in control of mRNA stability. Academic Press, New York, NY.
10. **Datsenko KA, Wanner BL.** 2000. One-step inactivation of chromosomal genes in *Escherichia coli* K-12 using PCR products. Proc. Natl. Acad. Sci. U. S. A. **97**:6640–6645.
11. **Feng Y, Vickers TA, Cohen SN.** 2002. The catalytic domain of RNase E shows inherent 3′ to 5′ directionality in cleavage site selection. Proc. Natl. Acad. Sci. U. S. A. **99**:14746–14751.
12. **Froschauer EM, Kolisek M, Dieterich F, Schweigel M, Schweyen RJ.** 2004. Fluorescence measurements of free [Mg^{2+}] by use of mag-fura 2 in *Salmonella enterica.* FEMS Microbiol. Lett. **237**:49–55.
13. **Hmiel SP, Snavely MD, Miller CG, Maguire ME.** 1986. Magnesium transport in *Salmonella typhimurium*: characterization of magnesium influx and cloning of a transport gene. J. Bacteriol. **168**:1444–1450.
14. **Jaskiewicz L, Filipowicz W.** 2008. Role of Dicer in posttranscriptional RNA silencing. Curr. Top. Microbiol. Immunol. **320**:77–97.
15. **Jiang X, Diwa A, Belasco JG.** 2000. Regions of RNase E important for 5′-end-dependent RNA cleavage and autoregulated synthesis. J. Bacteriol. **182**:2468–2475.
16. **Kavalchuk K, Madhusudan S, Schnetz K.** 2012. RNase III initiates rapid degradation of *proU* mRNA upon hypo-osmotic stress in *Escherichia coli.* RNA Biol. **9**:0–1.
17. **Kehres DG, Lawyer CH, Maguire ME.** 1998. The CorA magnesium transporter gene family. Microb. Comp. Genomics **3**:151–169.
18. **Kehres DG, Maguire ME.** 2002. Structure, properties and regulation of magnesium transport proteins. Biometals **15**:261–270.
19. **Kim K, Sim SH, Jeon CO, Lee Y, Lee K.** 2011. Base substitutions at scissile bond sites are sufficient to alter RNA-binding and cleavage activity of RNase III. FEMS Micrbiol. Lett. **315**:30–37.
20. **Kime L, Jourdan SS, McDowall KJ.** 2008. Identifying and characterizing substrates of the RNase E/G family of enzymes. Methods Enzymol. **447**: 215–241.
21. **Kole R, Altman S.** 1979. Reconstitution of RNase P activity from inactive RNA and protein. Proc. Natl. Acad. Sci. U. S. A. **76**:3795–3799.
22. **Lee K, Bernstein JA, Cohen SN.** 2002. RNase G complementation of *rne* null mutation identifies functional interrelationships with RNase E in *Escherichia coli.* Mol. Microbiol. **43**:1445–1456.
23. **Lee K, Holland-Staley CA, Cunningham PR.** 2001. Genetic approaches to studying protein synthesis: effects of mutations at Psi516 and A535 in *Escherichia coli* 16S rRNA. J. Nutr. **131**:2994S–3004S.
24. **Lee K, Varma S, SantaLucia J, Jr, Cunningham PR.** 1997. *In vivo* determination of RNA structure-function relationships: analysis of the 790 loop in ribosomal RNA. J. Mol. Biol. **269**:732–743.
25. **Lee K, et al.** 2003. RraA, a protein inhibitor of RNase E activity that globally modulates RNA abundance in *E. coli.* Cell **114**:623–634.
26. **Lee Y, Han J, Yeom KH, Jin H, Kim VN.** 2006. Drosha in primary microRNA processing. Cold Spring Harb. Symp. Quant. Biol. **71**:51–57.
27. **Mackie GA.** 1998. Ribonuclease E is a 5′-end-dependent endonuclease. Nature **395**:720–723.
28. **Matsunaga J, Dyer M, Simons EL, Simons RW.** 1996. Expression and regulation of the *rnc* and *pdxJ* operons of *Escherichia coli.* Mol. Microbiol. **22**:977–989.
29. **McCall KA, Fierke CA.** 2000. Colorimetric and fluorimetric assays to quantitate micromolar concentrations of transition metals. Anal. Biochem. **284**:307–315.
30. **Nelson DL, Kennedy EP.** 1972. Transport of magnesium by a repressible and a nonrepressible system in *Escherichia coli.* Proc. Natl. Acad. Sci. U. S. A. **69**:1091–1093.
31. **Papp-Wallace KM, Maguire ME.** 2008. Regulation of CorA Mg^{2+} channel function affects the virulence of *Salmonella enterica* serovar Typhimurium. J. Bacteriol. **190**:6509–6516.
32. **Ramachandran V, Chen X.** 2008. Small RNA metabolism in *Arabidopsis.* Trends Plant Sci. **13**:368–374.
33. **Ranquet C, Ollagnier-de-Choudens S, Loiseau L, Barras F, Fontecave M.** 2007. Cobalt stress in *Escherichia coli.* The effect on the iron-sulfur proteins. J. Biol. Chem. **282**:30442–30451.
34. **Reed RE, Baer MF, Guerrier-Takada C, Donis-Keller H, Altman S.** 1982. Nucleotide sequence of the gene encoding the RNA subunit (M1 RNA) of ribonuclease P from *Escherichia coli.* Cell **30**:627–636.
35. **Regnier P, Portier C.** 1986. Initiation, attenuation and RNase III processing of transcripts from the *Escherichia coli* operon encoding ribosomal protein S15 and polynucleotide phosphorylase. J. Mol. Biol. **187**:23–32.
36. **Robertson HD, Webster RE, Zinder ND.** 1968. Purification and properties of ribonuclease III from *Escherichia coli.* J. Biol. Chem. **243**:82–91.
37. **Sermon J, et al.** 2005. CorA affects tolerance of *Escherichia coli* and *Salmonella enterica* serovar Typhimurium to the lactoperoxidase enzyme system but not to other forms of oxidative stress. Appl. Environ. Microbiol. **71**:6515–6523.
38. **Sim SH, et al.** 2010. *Escherichia coli* ribonuclease III activity is downregulated by osmotic stress: consequences for the degradation of *bdm* mRNA in biofilm formation. Mol. Microbiol. **75**:413–425.
39. **Snavely MD, Gravina SA, Cheung TT, Miller CG, Maguire ME.** 1991. Magnesium transport in *Salmonella typhimurium.* Regulation of *mgtA* and *mgtB* expression. J. Biol. Chem. **266**:824–829.
40. **Soncini FC, Garcia Vescovi E, Solomon F, Groisman EA.** 1996. Molecular basis of the magnesium deprivation response in *Salmonella typhimurium*: identification of PhoP-regulated genes. J. Bacteriol. **178**:5092–5099.
41. **Thorgersen MP, Downs DM.** 2007. Cobalt targets multiple metabolic processes in *Salmonella enterica.* J. Bacteriol. **189**:7774–7781.
42. **Tock MR, Walsh AP, Carroll G, McDowall KJ.** 2000. The CafA protein required for the 5′-maturation of 16 S rRNA is a 5′-end-dependent ribonuclease that has context-dependent broad sequence specificity. J. Biol. Chem. **275**:8726–8732.
43. **Wang W, Bechhofer DH.** 1997. *Bacillus subtilis* RNase III gene: cloning, function of the gene in *Escherichia coli*, and construction of *Bacillus subtilis* strains with altered rnc loci. J. Bacteriol. **179**:7379–7385.
44. **Xiao J, Feehery CE, Tzertzinis G, Maina CV.** 2009. *E. coli* RNase III(E38A) generates discrete-sized products from long dsRNA. RNA **15**: 984–991.
45. **Xu W, Huang J, Cohen SN.** 2008. Autoregulation of AbsB (RNase III) expression in *Streptomyces coelicolor* by endoribonucleolytic cleavage of *absB* operon transcripts. J. Bacteriol. **190**:5526–5530.
46. **Yamamoto K, Ogasawara H, Fujita N, Utsumi R, Ishihama A.** 2002. Novel mode of transcription regulation of divergently overlapping promoters by PhoP, the regulator of two-component system sensing external magnesium availability. Mol. Microbiol. **45**:423–438.
47. **Yeom JH, et al.** 2008. Inhibitory effects of RraA and RraB on RNAse E-related enzymes imply conserved functions in the regulated enzymatic cleavage of RNA. FEMS Microbiol. Lett. **285**:10–15.
48. **Yeom JH, Lee K.** 2006. RraA rescues *Escherichia coli* cells over-producing RNase E from growth arrest by modulating the ribonucleolytic activity. Biochem. Biophys. Res. Commun. **345**:1372–1376.